Video Article

Subsurface Defect Localization by Structured Heating Using Laser Projected Photothermal Thermography

Erik Thiel[1], Mathias Ziegler[1]

[1]Department for Non-Destructive Testing, Thermographic Methods, Bundesanstalt für Materialforschung und -prüfung (BAM)

Correspondence to: Mathias Ziegler at mathias.ziegler@bam.de

Abstract

The presented method is used to locate subsurface defects oriented perpendicularly to the surface. To achieve this, we create destructively interfering thermal wave fields that are disturbed by the defect. This effect is measured and used to locate the defect. We form the destructively interfering wave fields by using a modified projector. The original light engine of the projector is replaced with a fiber-coupled high-power diode laser. Its beam is shaped and aligned to the projector's spatial light modulator and optimized for optimal optical throughput and homogeneous projection by first characterizing the beam profile, and, second, correcting it mechanically and numerically. A high-performance infrared (IR) camera is set up according to the tight geometrical situation (including corrections of the geometrical image distortions) and the requirement to detect weak temperature oscillations at the sample surface. Data acquisition can be performed once a synchronization between the individual thermal wave field sources, the scanning stage, and the IR camera is established by using a dedicated experimental setup which needs to be tuned to the specific material being investigated. During data post-processing, the relevant information on the presence of a defect below the surface of the sample is extracted. It is retrieved from the oscillating part of the acquired thermal radiation coming from the so-called depletion line of the sample surface. The exact location of the defect is deduced from the analysis of the spatial-temporal shape of these oscillations in a final step. The method is reference-free and very sensitive to changes within the thermal wave field. So far, the method has been tested with steel samples but is applicable to different materials as well, in particular to temperature sensitive materials.

Video Link

The video component of this article can be found at https://www.jove.com/video/55733/

Introduction

The laser projected photothermal thermography (LPPT) method is used to locate subsurface defects that are embedded in the volume of the test specimen and oriented predominantly perpendicular to its surface.

The method uses the destructive interference of two anti-phased thermal wave fields of the same elongation and frequency as shown in **Figure 1b**. In isotropic defect-free materials, the thermal waves neutralize destructively (*i.e.* zero temperature oscillation) at the symmetry plane by coherent superposition. In case of a material with a subsurface defect, the method takes advantage of the interaction of the lateral (*i.e.* in-plane) components between the transient heat flow and this defect. This interaction can be measured in a recreated oscillating temperature elongation at the symmetry line on the sample surface. Now, the defect containing sample is scanned by the superposed thermal wave field and the level of temperature elongation is measured in relation to the sample position. Due to symmetry, the destructive interference condition is satisfied once again when the defect crosses the symmetry plane; this enables us to locate the defect very sensitively. Moreover, since the level of maximal disturbance of the destructive interference correlates with the depth of the defect, it is possible to determine its depth by analyzing the temperature scan[1].

The LPPT can be assigned to the active thermography methodology, a well-established non-destructive method, where transient heating is actively generated and the resulting, also transient, temperature distribution is measured via a thermal IR camera. In general, the sensitivity of this methodology is limited to defects which are oriented essentially perpendicular to the transient heat flow. Moreover, since the governing transient heat conduction equation is a parabolic partial differential equation, the heat flow into the volume is strongly damped. As a consequence, the probing depth of the active thermography methodology is limited to a near surface region, usually in the millimeter-range. Two of the most common active thermography techniques are pulsed and lock-in thermography. They are fast due to planar optical surface illumination[2], but lead to a transient heat flow perpendicular to the surface. Therefore, the sensitivity of these techniques is limited to defects predominantly oriented parallel (*e.g.* delaminations or voids) to the heated sample surface. An empirical rule for pulsed thermography states that "the radius of the smallest detectable defect should be at least one to two times larger than its depth under the surface"[3]. To increase the effective interaction area between a perpendicularly oriented defect (*e.g.* a crack) and the heat flow, the direction of the heat flow needs to be

changed. Local excitation, by using a focused laser with a linear or circular spot for instance, generates a heat flow with an in-plane component that is able to effectively interact with the perpendicular defect[4,5,6,7].

In the presented method, we also use the lateral heat flow components to detect subsurface defects, but we use the fact that thermal waves can be superposed, whereas defects, especially vertically oriented ones, disturb this superposition. In this way, the presented method resembles a reference-free, symmetric and very sensitive method, as it is possible to detect artificial subsurface defects at a width/depth ratio of far below one[8,9]. Until now, it was difficult to create two anti-phased thermal wave fields supplying sufficient energy. We achieved this by coupling a spatial light modulator (SLM) to a high-power diode laser, which enabled us to merge the high optical power of the laser system with the spatial and temporal resolution of the SLM (see **Figure 2**) into a high-power projector. The thermal wave fields are now created by photothermal conversion of two anti-phased sinusoidally modulated line patterns via the pixel brightness of the projected image (see **Figure 2**, **Figure 1a**). This leads to structured heating of the sample surface and results in well-defined destructively interfering thermal wave fields. In order to find a subsurface defect, the disturbance of the destructive inference is measured as a temperature oscillation at the surface using an IR camera.

The term thermal wave, is controversially discussed because thermal waves do not transport energy due to the diffusive character of the heat propagation. Still, there is wave-like behavior when heating periodically, allowing us to use similarities between real waves and diffusion processes[10,11,12]. Thus, a thermal wave can be understood as highly damped in the propagation direction but periodic over time (**Figure 1b**).

The characteristic thermal diffusion length $\mu = \sqrt{k/(\pi f \rho c_p)}$ is hereby described by its material properties (thermal conductivity k, heat capacity c_p and density ρ), and the excitation frequency f. Although the thermal wave is decaying strongly, its wave nature can be applied to gain insight into the properties of the sample. The first application of thermal wave interference was used to determine the thickness of layers. In contrast to our method, the interference effect was used in the depth dimension (*i.e.* perpendicular to the surface)[13]. Extending the idea of interference to a second dimension by splitting up a laser beam, thermal wave interference was used to size subsurface defects[14]. Still this method was applied in transmission configuration, which means that it was limited by the penetration depth of the thermal wave. Furthermore, because only one laser source has been used, this method applies constructive interference, meaning that a defect-free reference is needed. Apart from the idea of using thermal wave interference, the first technical approach to spatially and temporally controlled heating was performed by Holtmann *et al.* using an unmodified liquid crystal display (LCD) projector with the built-in light source, which was severely limited in its optical output power[15]. Further approaches by Pribe and Ravichandran aimed at increasing the optical output power by also coupling a laser to a SLM[16,17].

The protocol presented herein describes how to apply the LPPT method to locate subsurface defects oriented perpendicularly to the surface of steel samples. The method is at an early stage, yet powerful enough to validate the proposed approach; however, it is still limited in terms of the achievable optical output power of the experimental setup. Since the increase of the optical output power remains a challenge, the presented method is applied to coated steel containing artificial electrically discharge machined notches. Nevertheless, the most important and most critical steps of the protocol, generating a homogeneous structured illumination, meeting prerequisites for destructive thermal wave interference, and locating the defect, still hold for more demanding defects as well. Since the governing quantity is the thermal diffusion length μ, the LPPT method can be applied to numerous different materials as well.
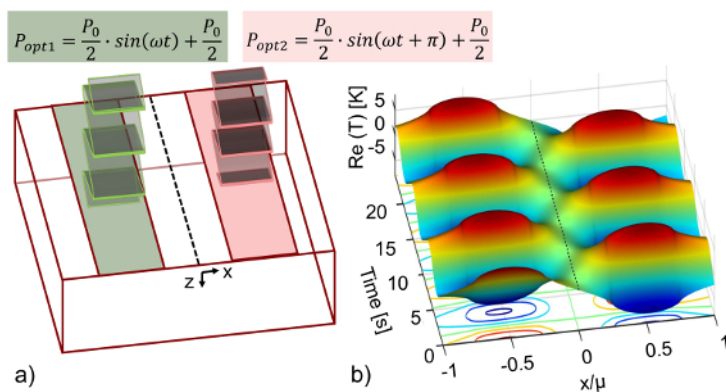
Figure 1: Principle of destructive interference effect. (**a**) Schematic of the illumination pattern used during experiments. The sample is spatially and temporally heated by two periodically illuminated patterns with a phase shift of π. The dashed line represents the symmetry line between both patterns. This line will be used for evaluation as a "depletion line". (**b**) Diagram of the spatially and temporally resolved alternating thermal result as calculated from the analytical solution of the thermal heat conduction equation. It shows the responding thermal waves to the illumination of (a) with an irradiance of the two patterns with P_{opt1} = 1.5 W sin(2π 0.125 Hz t) + 1.5 W and P_{opt2} = 1.5 W sin(2π 0.125 Hz t + π) + 1.5 W for constructional steel ρ = 7,850 kg/m^3, c_p = 461 J/(kg·K), k = 54 W/(m·K). The temperature profile at the dashed line shows no thermal oscillation for homogeneous, isotropic material. Please click here to view a larger version of this figure.

May 2017 | 123 | e55733 | Page 2 of 13
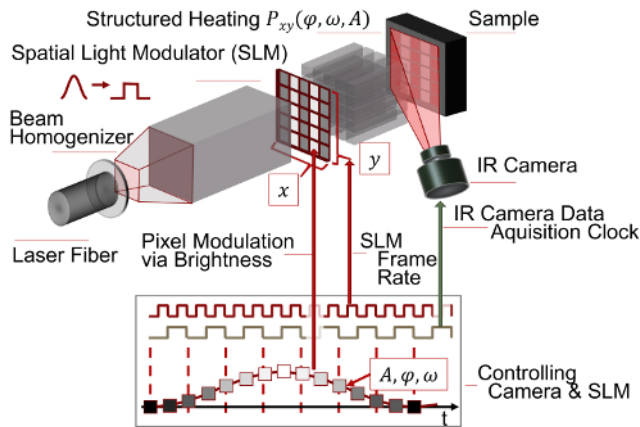
Figure 2: Schematic of the measurement principle of structured heating used in active thermography. A Gaussian beam homogenized to a top hat profile is applied to a Spatial Light Modulator (SLM). The SLM resolves the beam spatially by its switchable elements and temporally by its switching speed. Each element represents an SLM pixel. In this experiment, the SLM is a digital micro mirror device (DMD). By modulating the pixel brightness A with a time deterministic control software, the sample surface is heated in a structured way. In case of the presented experiment, we modulate two anti-phased lines (phases: $\varphi = 0, \pi$), which are the origin of coherently interfering thermal wave fields at the angular frequency ω. The wave fields interact with the sample's inner structure also influencing the temperature field at the surface. This is measured via its thermal radiation by a mid-wave infrared camera. Please click here to view a larger version of this figure.

Protocol

NOTE: Caution: Please pay attention to laser safety because the setup uses a class 4 laser. Please wear the correct protective glasses and clothes. Also, handle the pilot laser with care.

1. Couple the Diode Laser to the Projector Development Kit (PDK)

1. **Prepare the breadboard.**
   1. Preassemble all devices to the breadboard as shown in **Figure 3**. Place the breadboard with all preassembled devices in a laser laboratory.

2. **Position the laser fiber mount on the breadboard.**
   1. Attach the fiber to the laser fiber mount (*cf.* **Figure 3**).
   2. Switch shutter and laser threshold of the diode laser on. By using the high-power IR sensor card, check the output diameter (40 mm) of the beam. Switch the laser threshold off and the pilot laser on. Adjust the height of the optical axis at the laser fiber mount to the entrance of the PDK by using the lab jack (*cf.* **Figure 4a, 4d**).
   3. Move the laser fiber mount along the rail. Observe the position of the pilot laser at a distance. Its center point should not move. In case it does, check the mount between lab jack and laser fiber mount. Fix the laser fiber mount afterwards.
   NOTE: The rail is the reference for the optical axis and should be aligned parallel to the breadboard. The telescope lenses have to be removed beforehand.

3. **Adjust the telescope.**
   1. Use the telescope to reduce the beam diameter from 40 mm to 15 mm to fit into the entrance of the PDK (*cf.* **Figure 4a, 4d**). Use a 200-mm and a 75-mm plano convex lens as first and second lens, respectively. Use the pilot laser and the crosshairs to position the first lens (*cf.* **Figure 4b**).
   2. Roughly adjust the distance between both lenses using the steel ruler. Use the crosshairs again to position the lens to the pilot laser. Mount the second lens on to an xy translation stage. Use the stage to collimate the beam.

4. **Align the beam sampler.**
   1. Hit (with the laser beam) the beam sampler at an angle of 45°. Use a second rail perpendicular to the first to position the beam sampler.
   NOTE: Most of the optical power is cooled away by the 500 W power meter. The optical output of the diode laser is more stable at full power, which is why the optical power is split up.
   2. Use the iris in a height-fixed post to check the optical path way along the rail (*cf.* **Figure 4a**) with the pilot laser.

5. **Align the mirror.**
   1. Before aligning the mirror as shown in **Figure 4c**, remove the PDK and its base plate. Fix a third rail perpendicular to the second. Once again, check the optical path by the iris.
   NOTE: The optical path should be aligned to the rail orientation. The beam should be collimated.

6. **Disassemble and position the PDK.**
   1. Before positioning the PDK[18], remove the original light engine.

NOTE: There were two former lenses originally collimating the LEDs of the PDK[19] (*cf.* **Figure 4d**, entrance). They are glued and need to be removed by using acetone.

2. Align the platform of the PDK to be parallel to the third rail and therefore to the optical axis of the beam. Use the crosshairs adjusted to PDK's entrance to position the PDK relative to the beam. Stay aligned parallel. Switch the pilot laser off, because it is too weak to pass the PDK.

7. **Project a white image in order to check the optical power.**
   1. Make sure that HDMI-cable and USB-cable of the PDK as well as the data acquisition (DAQ) card are connected to the control PC. Connect the ports at the laser control box for "laser shutter", "laser threshold" and "laser on" to the DAQ card. Connect the "laser control voltage" port of the control box scanner to the DAQ card.
   2. Start the PDK control software[20] and configure it as an ordinary projector following the steps i.1 to i.3 of **Figure 5b**. Enable the second screen and make sure that there is no window within the second screen. Use a white desktop background and check the function of the projector with the LED flash light as input light source.
   NOTE: If a white image is projected to the image plane of the PDK, the device is working correctly.

8. **Check optical input power.**
   1. Put the 30 W power meter head attached to the power meter control unit in the optical path in front of the PDK (*cf.* **Figure 4e** - position 1). Switch the diode laser on with the LPPT laser control software following steps i.1 to i.3 of **Figure 5a**) at a low power level of step i.1 = 0.5 V.
   NOTE: The LPPT laser control software switches the DAQ card which switches the laser control outputs (*cf.* 1.7.1). Consider laser safety, wear glasses and protective clothes!
   2. Check the power meter sensor position with the high-power IR sensor card. Hold the IR card into the beam and watch it glow. Match the beam diameter to the power meter sensor area (**Figure 3**).
   3. Check the maximal optical input power at the entrance of the PDK (again follow **Figure 5a**), step i.1) with a value of 10 V.
   NOTE: The optical input power at the entrance of the PDK should be at maximum around 22 W[21]. At this configuration, measurement times up to 5 min were tolerated without destroying the SLM, which is in case of the PDK realized as a digital micromirror device (DMD).

9. **Check the optical output power.**
   1. Position the 30 W power meter head in an approximate distance of 60 mm to the PDK using a f = 60 mm lens attached to the PDK objective (*cf.* **Figure 4e**).
   2. Position the LED flash light at the entrance of the projector (*cf.* **Figure 4d**) and switch it on. Fine tune the position of the power meter head such that it collects the light of the projected image as shown in **Figure 4e**. Remove the LED flash light afterwards.
   3. Start the LPPT laser control software. Enter '0.5 V' into the "voltage" field and click the "Laser On!" button. Read the optical power from the power meter control unit. Stop the laser by clicking the "Stop" button. Repeat these steps for 2 V, 6 V, 10 V (*cf.* **Figure 5a**, i.1 to i.3).
   NOTE: If a voltage of 10 V provides an optical output power of >4 W, the initial test is successful. Else, the optical alignment needs to be checked. Try to maximize the optical output power by finely adjusting the mirror.

10. **Measure the beam profile.**
    1. Use a photo diode with amplifier and pinhole to measure the beam profile of the resulting projected image (*cf.* **Figure 4f**). If a beam profiler is accessible, use this device but weaken the beam.
    2. Attach the photo diode to a translation stage which is itself mounted to a bracket. Also attach a neutral-density (ND)1 reflective filter and the 1-mm pinhole to the diode. Place the photo diode on top of a motorized translation stage and the lab jack. To gain height, use two breadboards (100 mm x 100 mm).
    3. Use a f = 100 mm lens after the PDK-objective (*cf.* **Figure 4e**) and project a white image using the LED flash light (*cf.* step 1.7). Move the photo diode to the image plane and make sure that the range of the photo diode moving in translation stage is within the projected image (*cf.* **Figure 4f**).
    4. Connect the photo diode to the power supply and DAQ card. Use 40 dB amplification for 6 V control voltage for optical laser power. Connect the motion controller for the motorized translation stage to the control PC.
    NOTE: The LPPT intensity software controls the movement of the pinholed photo diode through the illuminated area at a constant velocity of v = 0.1 mm/s and records the photo diode signal at 100 kHz. The laser is also controlled via software.
    5. Use the micrometer screw of the stage in 1 mm steps as shown in **Figure 4f** in order to scan the image. See results shown in **Figure 6a-6b**.

11. **Calculate the correction image.**
    1. In order to correct the inhomogeneity of the beam profile, compute an inverted pixel matrix regarding the beam profile. Identify the range of the projected image using an edge detection algorithm.
    2. Transform time information into spatial information using the stage velocity. Transform the spatial information to the pixel domain of the PDK with x = 1,024 pixels and y = 768 pixels. Normalize the diode signal to the maximum value.
    NOTE: The reference level for correction was chosen with the mean of all normalized images values . The level of attenuation is computed with:

$$Pixel_{LC\,xy} = \frac{P_{mean}}{P_{pixel}}$$

P_{Pixel} is the normalized diode intensity per pixel. Values of $Pixel_{LC}$ above 1 are set to 1.
    3. Multiply the correction matrix (*cf.* **Figure 6c**) with a white image and measure the profile again in order to check if the correction was sufficient (*cf.* **Figure 6e-6h**).

2. Prepare the Sample

1. Use two blocks of 100 mm x 100 mm x 40 mm of constructional steel St37 as the sample material with a density of ρ = 7,850 kg m^{-3}, thermal conductivity k = 54 W·m^{-1}·K^{-1}, and heat capacity of c_p = 461 J·kg^{-1}·K^{-1}.
2. Insert artificial defects in two blocks at 0.25 mm, 0.5 mm, 0.7 mm, 1.25 mm and 1 mm, 1.5 mm, 1.75 mm, 2 mm by electrical discharge machining below the surface as shown in **Figure 7**.
3. Tape the defects with protective tape. Sandblast the top surface in order to have homogeneous absorption. Tape the defects with protective tape before coating. Degrease the surface using acetone.
4. Coat the illuminated area with graphite spray from 30 mm distance twice (0° and 90°). The coating is successful if there is a homogeneous surface. If the coating is not intact, start degreasing and cleaning again and repeat the coating step. Dry the surface ~2 h. Do not touch the surface, it will change emissivity.
5. Remove the tape and make sure that the graphite does not enter the subsurface defect.

3. Prepare the Experiment

1. **Prepare PDK and diode laser.**
   1. Project a white image as described in step 1.7). Check the optical input power of the PDK as described in step 1.8). Check the optical output power of the PDK as shown in step 1.9).
   2. Connect the 500 W power meter head to the power meter control unit and attach the power meter to the control computer (PC) via a USB-cable.

2. **Prepare the motion controller and position the sample.**
   1. Connect the motion controller to the translation stage and to the control computer via a USB-cable. Position the translation stage orthogonal to the optical axis at a distance of around 80 mm relative to PDK.
   NOTE: The LPPT software, running on the control computer controls the motion controller.
   2. Attach the f = 100 mm lens to the PDK objective. Use the LED flash light as input light source (*cf.* **Figure 4d**, the crosshairs mark the entrance) to the PDK to find the image plane of the projector.
      1. Position a white sheet of paper at an approximate distance of 100 mm in front of the objective and move it back and forth to find the plane of the sharp illuminated rectangle, which is the image plane.

   3. Position the coated sample surface at this plane. Set the height of the sample using the lab jack mounted to the linear translation stage. Choose the height such that the top of the illuminated rectangle hits the top of the sample (*cf.* **Figure 4g**). Position the defect that it is within range of the illuminated area.
   4. Zero the motion controller by switching the device off and on again.

3. **Prepare the camera and position the gold mirror.**
   1. Use the LED flash light as input light source for the projector to project a white image to the sample.
   2. Place the gold mirror at a height such that it sees the upper edge of the sample (**Figure 4g**). Set the mirror on an angle of about 35° as it is shown in **Figure 3**. Position the gold mirror as close as possible to the PDK objective but not shadowing the projection.
   NOTE: The mirror is attached to a post in a mounted post holder. The height and position are fixed by clamps.
   3. Mount the IR camera to the tripod. Level the IR camera with the bullseye level. Adjust the IR camera to the height of the PDK objective. Position it such that it sees the projected white image over the gold mirror.
   NOTE: The approximate distance along the optical pathway is around 1 m.
   4. Use the spacer ring in between the IR camera objective and the IR camera. Make sure that the trigger input of the camera is connected to the measurement data acquisition card in order to trigger the frame grabbing. Also, connect the IR camera control PC to the IR camera via LAN cable.
   5. Switch on the camera and wait at least for the warm-up time (*ca*. 30 min).
   6. Start IR camera control software. Change the menu bar item to "Camera". Click the "Connect" button to connect the IR camera (*cf.* **Figure 8a**, step i.1).
   NOTE: The camera shows a live image of the scene.
   7. Click the "Remote" button to open the panel "Remote Control" (*cf.* **Figure 8d**, step i.2). Choose the calibration "HF 100mm (-10 °C - 60 °C) 1140 µs". See **Figure 8d**, step i.2.1.
   NOTE: The calibration range should be as small as possible in order to reduce noise.
   8. Manually adjust the lens focus ring to focus the IR camera to the sample plane.
   NOTE: It is important that the camera's field of view is as big as the maximal projected area in order to have the maximal spatial resolution (*cf.* **Figure 4g**). One may have to change position, height and orientation of the IR camera. In order to decide if an image is sharp, one needs a temperature contrast at the image plane. A steel ruler may be used to generate a contrast. If the IR image still has low contrast, one may adjust it by using the selection tool (*cf.* **Figure 8c**, i.3)
   9. Perform a non-uniformity correction by clicking the button "NUC" (*cf.* **Figure 8d**, step i.2.2). Cover the IR camera objective and click the button "ok".

4. **Determine the relationship between IR camera pixel domain and projector coordinates.**
   1. Determine the relationship between the PDK pixel domain, the IR camera pixel domain and the length scale of the sample by projecting a white image or pattern to the sample surface (*cf.* **Figure 4 g, h**). Measure the projected area by using a steel ruler which gives the relation between the PDK domain and the length scale of the sample.
   2. Use the f = 100 mm lens attached to the PDK-objective in order to get an illuminated area of 21.3 mm x 16 mm (4:3).
   NOTE: The length scale in PDK coordinates is: 1 projected pixel = 21.3 mm/1,024 pixel
   3. Find the relationship between PDK and IR camera. Repeat step 1.9.3) for 10 V.

---

1. Use the IR camera software to change the menu bar item to "Measure". Choose the "Cross tool" from the "Measure areas" tool bar (*cf.* **Figure 8c**), step i.4). Mark the corners of the resulting thermal image by left clicking on the frame shown.
2. Right click on the cross to get to the property window. Change to "coordinates" and record them for later transformation of the thermal image to the PDK coordinate system.

4. Implement the Experiment

1. **Prepare the experiment.**
   1. Estimate illumination area relative to length scale of the sample.
      1. Use the f = 100 mm lens to obtain an illuminated area of 5.5 mm x 16 mm per pattern. Choose an area of 5.5 mm x 16.5 mm in between them which is not illuminated.
      NOTE: The resulting irradiance is approximately 1.2 W/cm².
   2. Estimate illumination area in units relative to the PDK pixel domain.
      1. Transform the illuminated pattern position to the PDK's pixel domain (1,024 pixels x 768 pixels) using the equation in step 3.4.2). Use [(512, 1); (512, 768)] pixels in the PDK domain as the depletion line, which is symmetric between both patterns.
   3. Compute total number of frames, measurement time and frames per period. Assuming a velocity of v = 0.05 mm/s, a stage travelling distance of x = 10 mm and a PDK frame rate fr = 40 Hz, compute the measurement time t via $t = x/v$ = 200 s. Also, compute the number of frames $nof = fr \cdot t$ = 8,000. With an excitation frequency of f = 0.125 Hz, compute the frames per period p with $p = nof/tf$ = 320 frames/period. These values will be used to generate the projected images.
   Note: These values will be used to generate the projected images.
   4. Check the setup and make sure that the laser system, the IR camera and (optionally) the temperature control is connected to the DAQ card. Check if the 500 W power meter, PDK and linear stage are connected to the control PC.

2. **Set up the camera control PC.**
   1. Configure the IR camera control software to grab a frame when the IR camera receives a trigger input. For this, switch to the panel "Camera" and click the "Remote" button (*cf.* **Figure 8a**, step i.2) to open the remote control panel. Choose "Process IO" from the drop-down menu (**Figure 8d**, step i.2.3) and enable "Sync In" and "Gate" and close the menu.
   2. Open the acquisition menu by clicking at the bottom-right corner of the "Acquisition parameters" tab (*cf.* **Figure 8a**, i.5). Choose "Ext/Sync" from the drop down menu (*cf.* **Figure 8b**, i.5.1). Name the measurement by entering file and folder names into the "Folder" field (see **Figure 8b**, i.5.2).
   3. Enter the total frame number computed from step 4.1.3 into the "count" field (*cf.* i.5.3). Close the acquisition menu and click the "Record" button to start the IR camera data acquisition (*cf.* **Figure 8**, i.6).
   NOTE: The recording only will take place if there is a trigger input from the DAQ card.

3. **Perform the experiment.**
   1. Start the LPPT control software. Activate the motion controller by clicking the "Activate?" button (**Figure 9a**, i.1). Set the travelling parameters "StartPosition" = "-5 mm", "EndPosition" = "5 mm" and "Velocity" = "0.05 mm/s" by editing the corresponding named fields as shown in **Figure 9a**, i.1. Click the "Start Measurement" button (see **Figure 9a**, i.2).
   NOTE: In case it is unclear where the defect is located, choose a larger travelling distance at a higher speed. Pay attention to the increase in temperature of the PDK, and amount of data created. Note that a user interface for generating the frame images will appear (*cf.* **Figure 9b**).
   2. Generate the projected frame images.
      1. Left click on the "Choose Area Color" field. Choose a color for the pattern area from the color dialog (**Figure 9**, i.3). Choose the 'rectangle tool' from the drawing toolbar in the upper-left corner.
      2. Draw a rectangle on the image area by left clicking and holding while extending over the image area. Use the transformed pattern coordinates from step 4.1.2) to size the rectangle coordinates shown in the left bottom corner (i.4). Click the "define Area" button (**Figure 9b**, i.5).
      NOTE: The computed pixel coordinates in the PDK domain for 5.5 mm pattern size are: Rectangle 1 (x1 = 116, y1 = 1; x2 = 380, y2= 768), Rectangle 2 (x1 = 644, y1 = 1; x2 = 908, y2= 768). After clicking the button "define Area", a dialog for setting the pattern properties will appear.
   3. Set the pattern properties (**Figure 9c**, i.6).
      1. Choose "sine wave" from the drop down menu by left click on the field "Signal Type". Define the oscillation parameters by setting the fields "Phase Shift" to "0°", "Frequency" to "0.125 Hz" and "Amplitude" to "127" (phase shift of 0 for the first pattern and a phase shift of π for the second).
      2. Set the laser voltage to 10 V by inserting "10" to the field "Voltage". Paste 320 to the "Pics/period" field using the value from step 4.1.3). Push the "Next" button; this closes the panel.
      NOTE: The LPPT control software computes a periodical image stream at the resolution of the PDK. As a white pixel means maximum optical power and a black pixel zero power, two oscillating patterns are calculated. The gray value of the first pattern is computed with $P_1 = 127 \sin(2\pi\ 0.125\ \text{Hz}\ t) + 127$ and that of the second with $P_2 = 127 \sin(2\pi\ 0.125\ \text{Hz}\ t + \pi) + 127$ (see **Figure 2**, graph), whereas the time t is discretized to the chosen frame rate (*cf.* step 4.3.4).
   4. Create the second projected pattern.

1. Repeat steps 4.3.2) and 4.3.3) following the workflow of **Figure 9** but with a different color and a different "Phase Shift" of "180°". Click the "calc Frames" button to compute the projected patterns. Set the PDK and IR camera frame rate to be "40 Hz" in the popped up dialog box.

5. Load the correction image.
   1. Follow the workflow of **Figure 9b**), step i.12. Choose the "load correction" panel, and provide the file for the computed image from step 1.11). Load the correction image by clicking the button.

6. Start the measurement by clicking the "Start" button (*cf.* **Figure 9b**, step i.13).
   NOTE: The computed frames will be projected onto the sample while the stage is moving. The frames will be acquired and counted by the IR camera control software.

7. Stop the measurement when all frames are acquired (progress bar = 100 %) by clicking the "Stop Measurement" button (*cf.* **Figure 9a**, i.14).
   NOTE: The label of the button will change if clicked.

5. Post-process the Data File

1. Start the LPPT post-processing software. Click the "load" button and choose the measurement file in the file dialog box. Click "OK" to transform the camera data format to post-processing data format (*cf.* **Figure 10a**).
   NOTE: The IR camera data is stored at the IR camera control PC in a native format. The IR camera control software development kit is used to convert the IR camera sequence to a 3-dimensional matrix (pixel X, pixel Y, frame number) and a header including a timing vector t.

2. Transform the IR camera data to the PDK domain (*cf.* **Figure 10b**), by inserting the coordinates of the four projection points P1x to P4y from step 3.4.3), and clicking "Transform".
   NOTE: Due to the image projection via the gold mirror to the IR camera (*cf.* **Figure 4g**), the resulting IR image is distorted. An affine geometrical transformation is performed from the IR camera domain to the PDK domain. The result is a matrix of size 1,024 x 768 x frame number.

3. Extract temperature information at the depletion line (*cf.* **Figure 10c**).
   1. Define the depletion line with two points L1 and L2 by filling the fields L1x = Lx2 = "512" pixel as it was already chosen in step 4.1.2). Choose y from L1y = "343" to L2y = "393". See **Figure 10c**.
      NOTE: Due to the transformation in step 5.2), the data can be retrieved right away, but side effects occur because the sample is only partly illuminated. Therefore, do not evaluate the edge areas of the patterns. If the noise is still too high, the size of y can be increased.
   2. Set the experimental parameters for the IR camera by filling the following fields: FrameRate as "40" Hz, frequency as "0.125" Hz, velocity v as "0.05" mm/s and starting position xStart as "-5" mm (*cf.* **Figure 10c**). Set the parameters for data post-processing: "Fit Degree" = "7", "Smoothing" = "20", and "Hilbert" = "500" as in **Figure 10c**.
      NOTE: The data extracted at the depletion line is geometrically averaged. Afterwards, the alternating temperature term ΔT (see **Figure 11a, b**) is retrieved by performing a polynomial fit (Fit Degree). The resulting signal is smoothed by a moving average filter (Smoothing). Finally, a Hilbert transformation is applied in order to retrieve the instantaneous amplitude. Another moving average filter (Hilbert) is applied in order to reduce residual ripples. Using information on the amplitude minimum, the position of the hidden defect is obtained.
   3. Click "Evaluate" to perform the data analysis. Read the computed position of the defect from the field "CrackPosition [mm]".The defect position is shown in the window of **Figure 10d**.
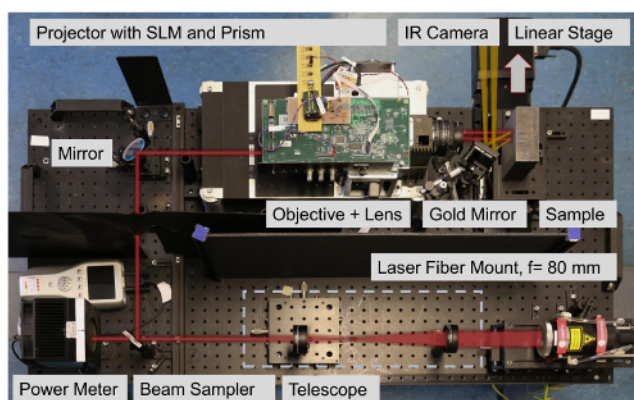
Figure 3: Photograph of the experimental setup with highlighted optical path (red line). The laser fiber mount is attached to the fiber of the diode laser. The beam is adjusted by the telescope to the entrance diameter of the PDK. Before entering the PDK, the beam is split by the beam sampler and monitored by the power meter. Inside the PDK, the beam is homogenized and projected to a DMD. The PDM, controlled by the LPPT control software, projects illumination patterns to the sample. The projected light is photothermally converted and heats up the sample. The temperature is measured by an IR camera via the thermal radiation (orange line) emitted from the sample surface. The sample itself is positioned on the linear translation stage. Please click here to view a larger version of this figure.
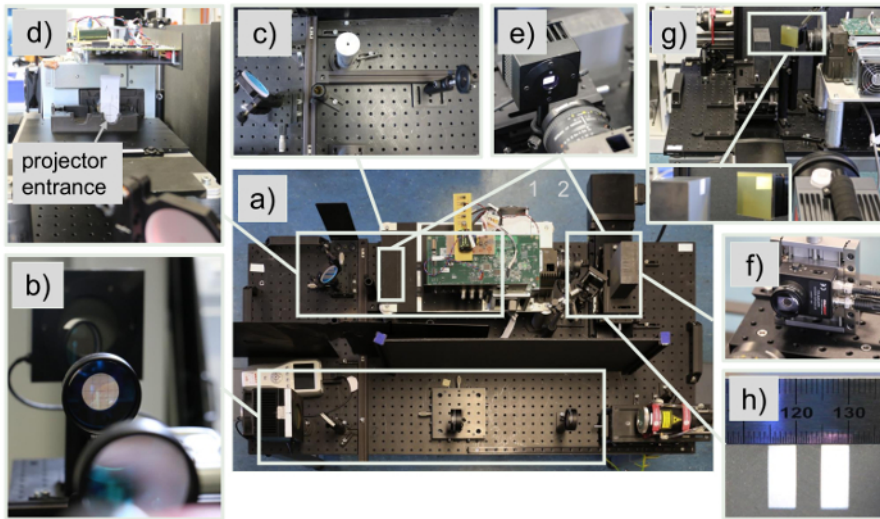
Figure 4: Photo sequence showing the adjustment of the experimental setup. (**a**) Top view of the experimental setup shows an overview. (**b**) Alignment of the telescope: The crosshairs are used to center the lens to the optical axis of the laser beam. (**c**) Aligning the optical elements: A bar system mounted to the optical bench is used to align the optical beam relative to the bench. A height fixed iris is used to keep the beam parallel to the bench. (**d**) Photo of the side view of the coupling point between projector and beam. The crosshairs are used to align the projector to the beam. (**e**) Determining the transmission of the projector system: The power meter is used to measure the optical power before and after the projector. (**f**) Determination of the beam profile: Pinhole and ND1 filter are mounted to the diode which is moved via two linear stages through the projected image. The projector has to be configured to project a white image. (**g**) Positioning of the infrared camera to the sample via a gold mirror: The sample has to be positioned in the image plane of the projector. In order to control the power density, the objective and additional lenses attached to the objective can be used. (**h**) Determination of the scale between projected image, IR camera image and the actual length of the sample. Please click here to view a larger version of this figure.
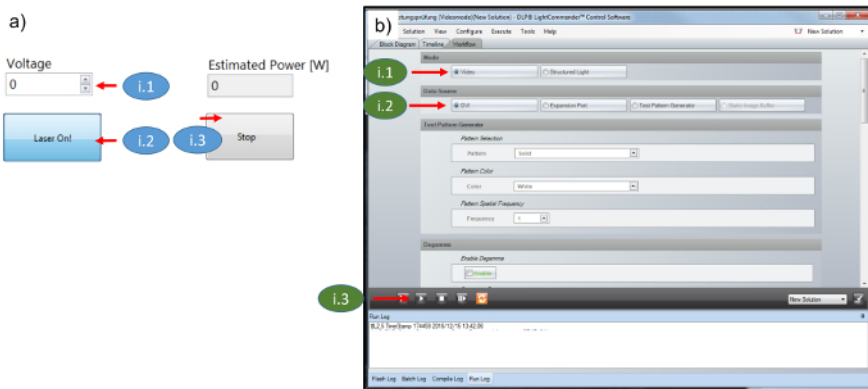

Figure 5: Software screenshots. (**a**) Screenshot of LPPT laser control software. (**b**) PDK control software: Steps i.1 to i.3 show how to configure the PDK as an ordinary projector. Please click here to view a larger version of this figure.
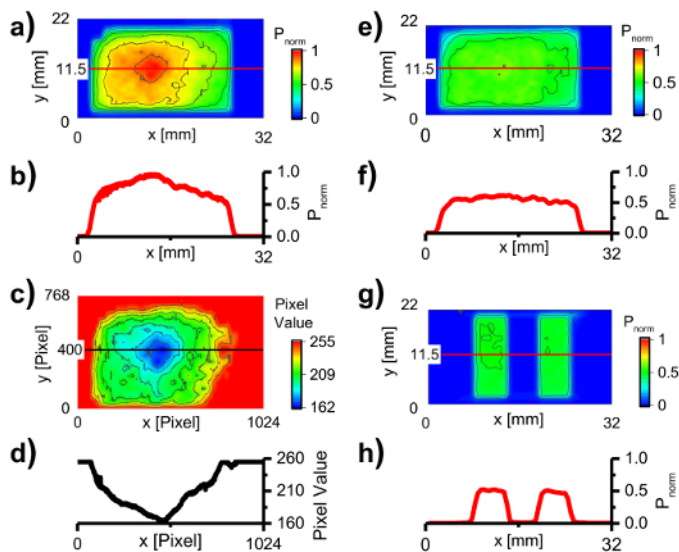
Figure 6: Correction of the inhomogeneous beam profile. (a) Beam profile of the projected white image (full illumination) taken by a photo diode which was moved through the profile. The data shows an inhomogeneous beam profile with a prominent peak in the middle. (b) The cross section line profile corresponding to the red line in a). (c) Correction image which is overlaid on the SLM with the projected white image in order to reduce the level of inhomogeneity. (d) The corresponding cross section line profile of the red line in c). (e) Resulting beam profile after correction showing a profile closer to a top hat profile. (f) The corresponding cross section line profile of the red line in e). (g) Illumination profile of two corrected patterns. The patterns will be modulated with the same frequency and amplitude but with opposing phases creating a zone of destructive interference in between the patterns. (h) The corresponding cross section line profile of the red line in g). Please click here to view a larger version of this figure.
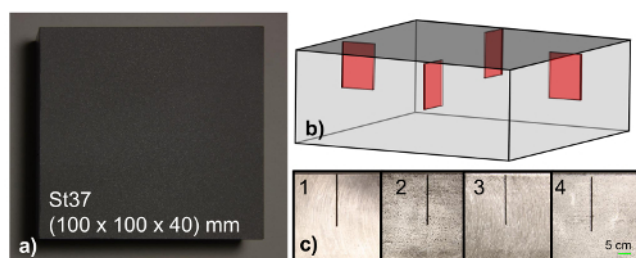

Figure 7: Sample preparation. (a) Photograph of the sample surface showing a block of black coated structural steel St37 (20 mm x 0.5 mm x 15 mm). (b) Transparent CAD drawing of the subsurface defects. The defects are located 40 mm from the right side. (c) Side view photos of the samples showing the idealized defects at different depths beneath the surface (side 1 = 0.25 mm, side 2 = 0.5 mm, side 3 = 0.7 mm, side 4 = 1.25 mm). The sample sides are uncoated in order to reduce heat losses. The second sample (not shown) has its subsurface defects at: side 1 = 1 mm, side 2 = 1.5 mm, side 3 = 1.75 mm, side 4 = 2 mm. Please click here to view a larger version of this figure.
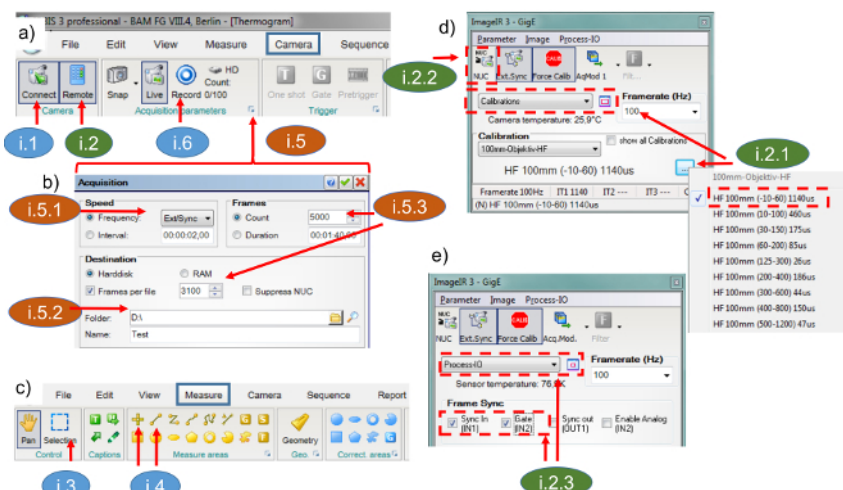

Figure 8: Screenshots of the IR camera control software. Steps i.1 to i.5 show how to configure the IR camera for data acquisition. (a) Screenshot of "Camera" panel: the IR camera can be connected to the IR camera control PC via the "Connect" button. The "Remote" control

panel (b) and the acquisition panel (d & e) can be reached from here. Furthermore, the measurement can be started via the "Record" button. (**b**) Screenshot of the "Acquisition" panel: the IR camera needs to be configured via "Ext/Sync" in order to capture a frame if it receives a 5 V TTL trigger. (**c**) Screenshot of "Measure" panel: the data display range can be adjusted by the "Selection" button. Point and Line tools are used to calibrate the IR camera image to real world coordinates. (**d**) Screenshot of IR camera remote control "Calibrations" panel. A small measurement range (-10 to 60 °C) has to be chosen in order to achieve a high sensitivity. (**e**) IR camera remote control panel: "Process-IO", "IN1" and "IN2" have to be enabled in order to trigger the IR camera. Please click here to view a larger version of this figure.
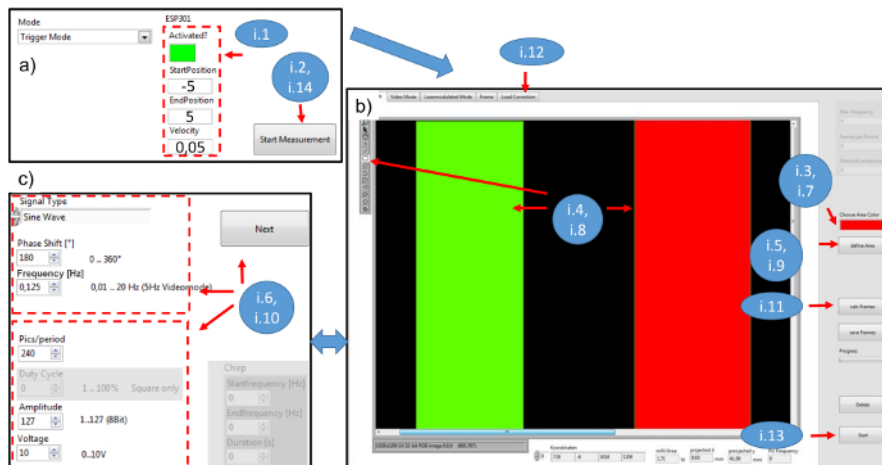
Figure 9: Screenshots of the LPPT control software. The workflow for user interactions with the software is marked with as steps i.1 to i.14. (**a**) Screenshot of the LPPT main panel; "Activated?" is a Boolean type and activates the stage if true. "Start-" and "EndPosition" are the travel parameters of the stage in mm. The field "Velocity" is defined in mm/s. The "Start Measurement" button starts measurements, opens the dialog box shown in panel (b) and stops the measurement if false. (**b**) Screenshot of the user interface used to create the patterns projected to the sample. A color is chosen to represent an area of pixels. The area is chosen by drawing rectangles to the image. If the button "define Area" is pressed, the panel shown in panel (c) will pop up to define the properties of the area. After defining all areas, the button "calc Frames" will compute a set of images. "Load Correction" will provide a dialog box to load the correction image to avoid an inhomogeneous beam profile. The button "Start" will start the measurement. (**c**) Screenshot of the user interface used to set the properties of one pattern. The upper frame shows signal type (sine wave), phase shift in degrees and frequency in Hz. The lower frame shows frames per period, amplitude from 1 to 127 and laser voltage (0 V to 10 V = 0 W to 500 W). Frames per period is the value representing how finely a period is discretized. After the button "Next" (further) is pushed, a dialog box pops up and asks for camera frame rate in Hz and frame switching speed in Hz. Please click here to view a larger version of this figure.
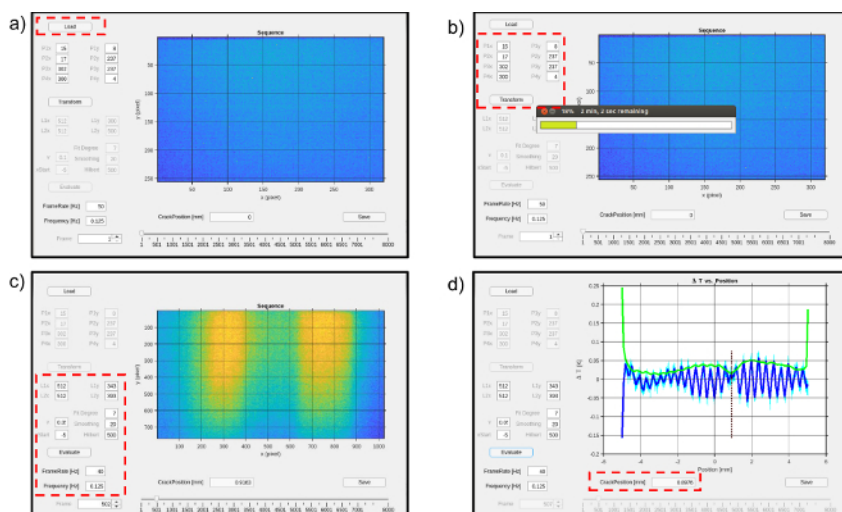
Figure 10: Screenshots of the LPPT post-processing software. (**a**) Load and transform the native IR camera data format. (**b**) Transform the frame matrix to the projectors coordinate system by using the transformation points P1x to P4y. (**c**) L1x to L2y represent the pixel coordinates of the evaluated line. "v", "xStart", "FrameRate" and "Frequency" are experimental parameters. "v" is the velocity in mm/s, "xStart" the starting position of the stage in mm, "FrameRate" and "Frequency" are given in Hz. "Fit Degree", "Smoothing" and "Hilbert" are evaluation parameters. Fit Degree represents the degree of the polynomial fit, "Smoothing" represents the number of elements for a moving average filter used to reduce noise and the "Hilbert" parameter is used to set the level of smoothing to find the minimum of the curve. (**d**) Screenshot of the result showing the crack position as a vertical dotted line. Please click here to view a larger version of this figure.
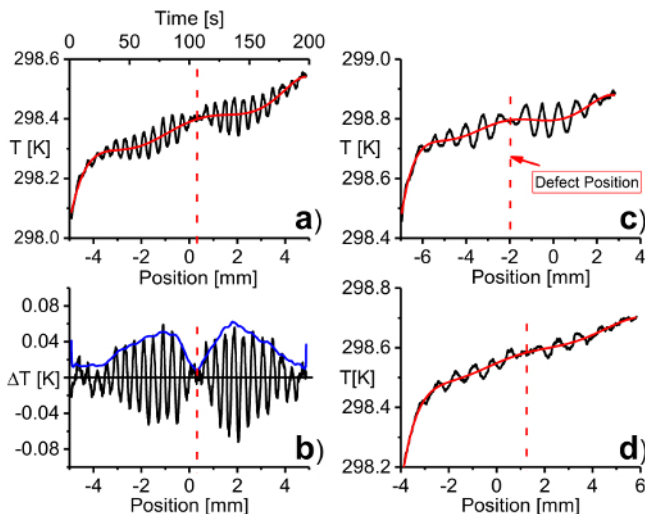
Representative Results

Following the protocol, side 1 of the steel sample with a subsurface defect at a depth of 0.25 mm was chosen to generate representative results. The defect was initially positioned approximately at the center of the illuminated area. The sample was then moved from -5 mm to 5 mm via the linear stage at a speed of 0.05 mm/s. Using these parameters, **Figure 11a** shows the scan data after extracting them from the depletion line. At this stage, the success of the experiment can be estimated, as the raw data is available from the IR camera control software as a preview (optional: Use the line tool to preview the data, *cf.* **Figure 8**, step i.4). Following further signal post-processing, **Figure 11b** shows the defect position at the minimum of the Hilbert curve (blue) at 0.3 mm.

To validate the experiment, the curve should have the following properties: it should be symmetrical, have a pronounced minimum at the symmetry plane and two equal maxima to its left and right. The maxima arise because the heat flow from one of the line sources dominates over the other due to the accumulation of heat at the defect. This is especially the case when the defect is positioned close to the symmetry plane. The defect forms a barrier for the heat flow so we can observe the heat flow of the dominating source and its reflection from the defect. If the defect is positioned symmetrically in the middle, the heat flow splits up equally, which results in a minimum[1].

The effect of the scan speed is shown in **Figure 11c**. Here, the scan speed was doubled to 0.1 mm/s to evaluate the same defect. Beforehand, the sample was shifted slightly on the stage in order to gain a different relative position. The defect position was determined to be -2 mm. The level of elongation was similar to the data shown in **Figure 11a**, demonstrating good reproducibility of the experiment, but with fewer oscillations. Since the maximal elongation correlates with the depth of the defect, information about position and depth can be maintained as well[1].

Figure 11d shows a suboptimal dataset. The defect was 1 mm below the surface, which is almost at the detection limit of this diffusion length and the available optical power. Although the location of the defect can still be determined, the measurement uncertainty is larger because the location of the zero oscillation is already affected by noise. From this behavior, we can infer that the most obvious signs for a failure of the defect detection experiment are if the depletion line vanishes completely or if there is a strong asymmetrical behavior. This can be due to the following reasons: (i) the spatial resolution of the IR camera is not sufficient and the depletion line cannot be resolved properly, (ii) the noise of the camera is too high in comparison to the temperature rise, (iii) the illumination pattern is inhomogeneous and has not been corrected properly, (iv) the chosen stage velocity is too high, as compared to the modulation frequency of the illumination pattern, and (v) the thermal diffusion length (via the modulation frequency) is not adapted to the defect depth.

Figure 11: Representative dataset from experiments to locate subsurface defects. (**a**) Representative experimental data from the St37 sample, side 1 with a defect at a depth of 0.25 mm. The black line shows temperature information over time (top axis). By translating the stage at a velocity v = 0.05 mm/s, the position is retrieved (bottom axis). The red curve shows a polynomial fit (7th degree) used to gain the alternating temperature component. The dashed red line represents the position of the subsurface defect.(**b**) The black curve shows the alternating temperature graph obtained by subtracting the polynomial fit from the temperature data of panel (a). The blue curve was obtained by applying Hilbert transformation to the black curve and averaging. (**c**) Representative experimental data of the same side over a range of -7 mm to 3 mm at a stage velocity of 0.1 mm/s. The frequency is halved but the elongation is similar to panel (a). (**d**) Suboptimal experimental data acquired when the subsurface defect was at a depth of 1 mm. Please click here to view a larger version of this figure.

Discussion

The presented protocol describes how to locate artificial subsurface defects oriented perpendicular to the surface. The main idea of the method is to create interfering thermal wave fields which interact with the subsurface defect. The most important steps are (i) to combine an SLM with a diode laser in order to create two alternating high-power illumination patterns at the sample surface; these patterns are photothermally converted into coherent thermal wave fields, (ii) to let them destructively interfere whilst interacting with a subsurface defect, and (iii) to locate these defects from a surface scan of the dynamic temperature of the sample surface using a thermal imaging IR camera. Since only the relative oscillation of

the temperature around a slowly varying mean value and not the absolute temperature value is needed, this approach is extremely sensitive to hidden defects[1].

One of the most critical steps within the protocol is to establish sufficient homogeneity of the illumination beam profile when using an SLM-coupled laser source for structured heating (refer to step 1.10). The diode laser offers a high irradiance but has to be fed into the projector containing the SLM with the correct beam diameter and directionality. Due to slight unavoidable geometrical and spectral mismatches with the proprietary optical path within the projector, the generated image on the sample is distorted. Therefore, a numerical correction of the image intensity values controlling the projected image is performed with a referencing beam profile measurement. A second critical step for a successful experiment is to achieve a high spatial resolution of the IR image (refer to steps 3.3.7- 3.3.8). The depletion zone has to be sufficiently spatially resolved, else no depletion and therefore no defect position can be measured.

The nature of the applied thermal waves is a diffusion-like process that leads to a strong attenuation of their amplitude over a few millimeters only. We meet this intrinsic physical limitation by using a high-power diode laser as light source. The bottleneck of the current experimental setup is the thermal stress limit of the SLM[21], which means that only a fraction of the available laser power can be applied. Our current solution is to coat the sample surface with a black graphite coating. In the future, we expect setups with higher sensitivity using optimized light engines or even switchable direct laser arrays, such as high-power vertical-cavity surface-emitting laser (VCSEL) arrays[22].

The main difference between this method and the existing thermal imaging in non-destructive testing is the fact that we use the destructive interference of fully coherent thermal wave fields; which is possible only after having control over amplitude and phase of a set of individual light sources in a deterministic way. Within the existing thermographic methods, either a planar light source, controlled in the time domain, or a single focused laser spot, controlled in the spatial domain, is used. The major advantage of our approach is high sensitivity to defects lying perpendicular to the sample surface.

Thus far, only two individual light sources have been created. With the laser-coupled SLM we can, in principle, generate and control up to one million individual light sources - one million heat sources - on the sample surface. Clearly this approach opens up the possibilities of arbitrary thermal wave shaping in the long term and transfer techniques from ultrasound or radar to the field of active thermography, within physical limits. Once the irradiance challenge as stated above (*i.e.* optical power per projected pixel) is satisfactorily solved, even smaller defects located deeper below the surface should become detectable. So far, steel has been tested, but the method is very promising especially for plastics, compound material, and other sensitive materials, due to the low thermal stress applied.

Disclosures

The authors have nothing to disclose.

Acknowledgements

References

1. Thiel, E., Kreutzbruck, M., & Ziegler, M. Laser-projected photothermal thermography using thermal wave field interference for subsurface defect characterization. *Appl. Phys. Lett.* **109** (12), 123504 (2016).
2. Ibarra-Castanedo, C., Tarpani, J. R., & Maldague, X. P. V. Nondestructive testing with thermography. *Eur. J. Phys.* **34** (6), S91-S109 (2013).
3. Maldague, X. P. Introduction to NDT by active infrared thermography. *Mater. Eval.* **60** (9), 1060-1073 (2002).
4. Li, T., Almond, D. P., & Rees, D. A. S. Crack imaging by scanning pulsed laser spot thermography. *Ndt&E Int.* **44** (2), 216-225 (2011).
5. Lugin, S. Detection of hidden defects by lateral thermal flows. *Ndt&E Int.* **56** 48-55 (2013).
6. Li, T., Almond, D. P., & Rees, D. A. S. Crack imaging by scanning laser-line thermography and laser-spot thermography. *Meas. Sci. Technol.* **22** (3) (2011).
7. Pech-May, N. W., Oleaga, A., Mendioroz, A., & Salazar, A. Fast Characterization of the Width of Vertical Cracks Using Pulsed Laser Spot Infrared Thermography. *Journal of Nondestructive Evaluation.* **35** (2), 22 (2016).
8. Thiel, E., Kreutzbruck, M., & Ziegler, M. in *Proc. SPIE 9761.* eds M. R. Douglass, P. S. King, & B. L. Lee) Spie-Int Soc Optical Engineering (2016).
9. Thiel, E., Kreutzbruck, M., & Ziegler, M. in *Proc. WCNDT 2016.* 6, (2016).
10. Mandelis, A. *Diffusion-Wave Fields: mathematical methods and Green functions.* Springer-Verlag (2001).
11. Almond, D., & Patel, P. *Photothermal Science and Techniques.* Vol. 10 Chapman & Hall (1996).
12. Salazar, A. Energy propagation of thermal waves. *Eur. J. Phys.* **27** (6), 1349-1355 (2006).
13. Bennett, C. A., & Patty, R. R. Thermal wave interferometry: a potential application of the photoacoustic effect. *Appl. Opt.* **21** (1), 49-54 (1982).
14. Busse, G. Stereoscopic depth analysis by thermal wave transmission for nondestructive evaluation. *Appl. Phys. Lett.* **42** (4), 366 (1983).
15. Holtmann, N., Artzt, K., Gleiter, A., Strunk, H. P., & Busse, G. Iterative improvement of Lockin-thermography results by temporal and spatial adaption of optical excitation. *Qirt J.* **9** (2), 167-176 (2012).
16. Pribe, J. D., Thandu, S. C., Yin, Z., & Kinzel, E. C. Toward DMD illuminated spatial-temporal modulated thermography. *Proc. SPIE 9861.* (2016).
17. Ravichandran, A. *Spatial and temporal modulation of heat source using light modulator for advanced thermography.*, Missouri University of Science and Technology, (2015).
18. TexasInstruments. *DLP 0.55 XGA Series 450 DMD.* (2015).
19. TexasInstruments. *Application Note - DLP System Optics.* (2010).

20. LogicPD. *DLP LightCommander Control Software - User Manual.* (2011).
21. TexasInstruments. *White Paper - Laser Power Handling for DMDs.* (2012).
22. Moench, H. *et al.* High-power VCSEL systems and applications. *Proc. SPIE 9348.* **9348** (2015).